

Spatiotemporal resolution for turbulent pipe flow simulations

Daniel Feldmann*

16th January 2020

1 Range of scales in turbulent pipe flow

A turbulent flow field is constituted of many irregular eddies and structures of many different sizes which all move and deform with different speed. Figure 1 shows instantaneous snapshots of a velocity field in a pipe to give an idea of the range of different length scales of these eddies. Comparing the contour plots for different Reynolds number also demonstrates how this spectrum of scales becomes even larger with increasing Re . Figure ?? shows time series

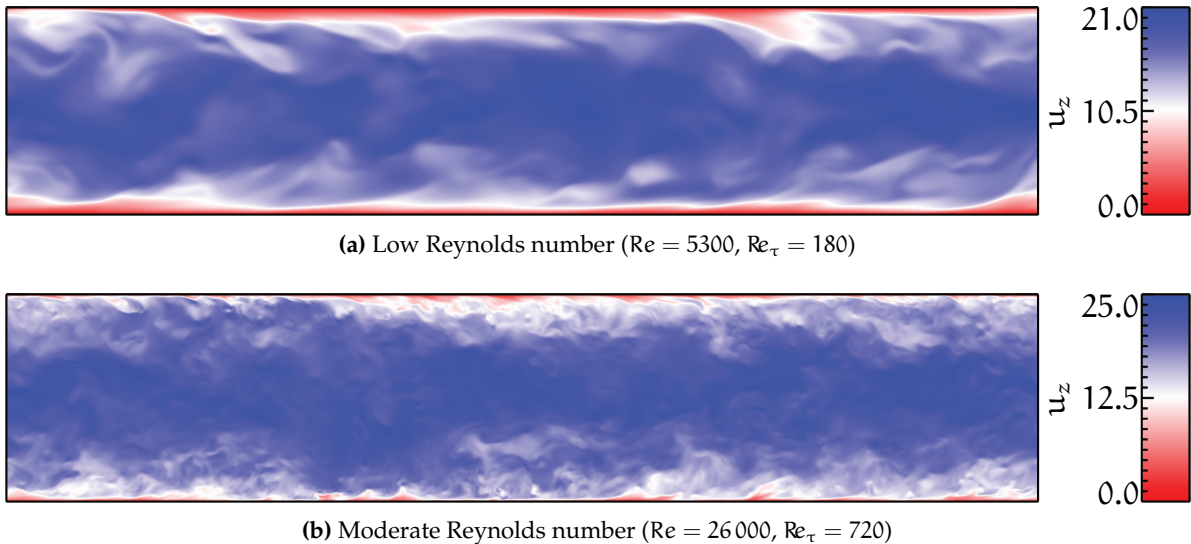


Figure 1: Comparison of turbulent pipe flow at two different Reynolds numbers to illustrate the huge range of different length scales of eddies and structures in the flow field. Shown are colour encoded contour plots of instantaneous snapshots of the streamwise velocity component (u_z) in a longitudinal section through the pipe taken from a DNS by Feldmann [2].

*University of Bremen, Center of Applied Space Technology and Microgravity (ZARM), Am Fallturm 2, 28359 Bremen, Germany, Email: daniel.feldmann@zarm.uni-bremen.de

of the streamwise velocity component $u_z(x, t)$ at given locations x to illustrate the huge range of time scales inherent to the turbulent flow field and its eddies and structures.

In a direct numerical simulation (DNS) the number of spatial grid points is determined by two constraints: First, the size of the computational domain must be large enough to accommodate the largest scale of turbulent motion. Here, the size can only be the length L of the pipe domain in axial direction, since there are natural constraints in azimuthal as well as in radial direction, which are inherent to the pipe geometry. Second, the grid spacing must be sufficiently fine to resolve the dissipative length scale, which is on the order of the smallest scale of the turbulent motion. The cubed ratio of these two scales provides a rough estimate for the total number of grid points (N) necessary for sufficient spatial discretisation of the Navier-Stokes equations. Additionally, the size of the discrete time step which is used to advance the Navier-Stokes equations in time has to be small enough to resolve the fastest fluctuations in the flow field. To set-up a well-resolved DNS of turbulent pipe flow for a given Re , the size of the smallest time and length scales has to be estimated a priori for this particular Reynolds number.

2 Kolmogorov scales

The characteristic scales of the smallest motions in a turbulent flow are the Kolmogorov scales, see e.g. Pope [4] page 185. These are the length (η), the time (τ_η), and the velocity (u_η) scales formed from dissipation rate ϵ and viscosity ν as follows:

$$\eta \equiv \left(\frac{\nu^3}{\epsilon} \right)^{1/4} \quad (1)$$

$$\tau_\eta \equiv \left(\frac{\nu}{\epsilon} \right)^{1/2} \quad (2)$$

$$u_\eta \equiv (\nu \epsilon)^{1/4}. \quad (3)$$

In preparation for a numerical simulation, the fluid property ν is in some or another way known or given, e.g. by the control parameter Re . The dissipation rate on the other hand, which is a property of the flow field and in general a function of space and time ($\epsilon = f(x, t)$), is a priori unknown and, therefore, has to be estimated to determine sufficient numerical resolution in advance. Figure ?? exemplarily shows dissipation rates calculated in a DNS at $Re_\tau = 720$ [].

3 Integral dissipation rate

Since $\epsilon(x, t)$ is never known in advance, one can roughly approximate (see e.g. Unger [6]) that

$$\epsilon(x, t) \approx \langle V \bar{\epsilon} \rangle_t, \text{ where } V \bar{\epsilon} = \iiint_V \epsilon(x, t) dV \quad (4)$$

represents a volume average over the entire computational pipe domain V . The integral dissipation rate plotted figure ?? makes clear how rough this estimate really is: Even in the temporal mean, dissipation in the pipe changes with distance from the pipe wall, i.e. $\langle \epsilon \rangle_t = f(r)$,

where r is the radial direction in the cylindrical pipe flow coordinate system. Near the pipe wall dissipation is larger than the integral value; in the bulk region dissipation is somewhat smaller. Surely there will also be instantaneous deviations from the temporal mean for all r which might be larger. We will see later, that this estimate is never the less very useful, if used carefully. Compare actual dissipation profiles (averaged and instantaneous) from DNS data later on to discuss this...

But the good thing is, that this integral value can be readily estimated from the pressure gradient

According to the unknown dissipation rate $\epsilon(x, t)$ can be approximated by the integral dissipation rate This quantity, in turn, can be readily estimated from the usually known pressure gradient $\langle dp/dz \rangle_t$ which drives the flow. This ansatz is based on the idea, that the total energy input to the system — basically the pressure gradient — is eventually dissipated into heat. Formally, this relation can be derived by integrating the time-averaged budget equation for the total kinetic energy and neglecting direct dissipation:

$$\left\langle \frac{dp}{dz} \right\rangle_t V u_b = \iiint_V \rho \epsilon(x, t) dV = \rho V \bar{\epsilon} V \quad (5)$$

$$\Rightarrow V \bar{\epsilon} = -\frac{1}{\rho} \left\langle \frac{dp}{dz} \right\rangle_t u_b. \quad (6)$$

In the Reynolds-averaged equations the pressure gradient and the wall-shear stress τ_w balances out

$$-\frac{1}{\rho} \left\langle \frac{dp}{dz} \right\rangle_t = \frac{4\tau_w}{D\rho} = \frac{4u_\tau^2}{D}. \quad (7)$$

From eq. (6) and eq. (7) it follows a simple relation

$$V \bar{\epsilon} = \frac{4u_\tau^2 u_b}{D} \quad (8)$$

for the a priori unknown integral dissipation, which is basically a function of u_τ and u_b , since the pipe diameter D is usually a known and constant quantity.

4 Shear to bulk velocity ratio

Usually, in pipe flow simulations either u_τ or u_b is a priori known while the other one is an observed quantity, depending how the flow is driven through the pipe in the numerical set-up. If the flow rate is kept constant during the simulation, usually the bulk Reynolds number

$$Re = \frac{\langle u_b \rangle_t D}{\nu} \quad (9)$$

based on the mean bulk flow velocity $\langle u_b \rangle_t$ is the relevant control parameter in the code. Thus, u_b is a known and constant quantity while u_τ is a result. If on the other hand, the driving force (i.e. the pressure gradient) is kept constant, usually the friction Reynolds number

$$Re_\tau = \frac{\langle u_\tau \rangle_t R}{\nu} = \frac{\langle u_\tau \rangle_t D}{2\nu} \quad (10)$$

based on the mean shear velocity $\langle u_\tau \rangle_t$ is the relevant control parameter in the code. Thus, $\langle u_\tau \rangle_t$ is a known quantity, while u_b is a result.

For further details and a comprehensive discussion on the different flow driving mechanisms in numerical simulations see e.g. Quadria et al. [5] and Hasegawa et al. [3], who also introduced a third alternative in which the power input to the system is kept constant and thus neither...

A well-known and by now well-established empirical relation between u_b and u_τ given by was first published by Blasius [1] in 1939 based on extensive experiments in turbulent pipe flow.

Friction law according to Blasius [1]

$$\lambda_{\text{Blasius}} = 0.3164 \cdot \text{Re}^{-1/4} \quad (11)$$

which is valid for $2300 \lesssim \text{Re} < 100\,000$. Darcy-Weisbach

$$p_2 - p_1 = \Delta p_{12} = \frac{\rho}{2} \frac{L \cdot \lambda}{D} u_b^2 \quad \text{with } \Delta z = L \quad (12)$$

$$\frac{\Delta p}{\Delta z} = \frac{\partial p}{\partial z} = \frac{\rho}{2} \frac{\lambda}{D} u_b^2 \quad (13)$$

5 Integral length scale

Using the integral dissipation rate given by eq. (8), from eq. (1) an integral (i.e. volume averaged) Kolmogorov length scale

$$\nu_{\bar{\eta}} = \left(\frac{\nu^3}{\overline{\nu \epsilon}} \right)^{1/4} = \left(\frac{D \nu^3}{4 u_b u_\tau^2} \right)^{1/4} \quad (14)$$

can be defined. For turbulent wall bounded flows it is common and convenient to express length scales in viscous units (also called wall or inner units) defined by

$$y^+ \equiv y \frac{u_\tau}{\nu} \quad (15)$$

and commonly denoted by $^+$. With eq. (15) and eq. (14) we arrive at

$$\begin{aligned} \nu_{\bar{\eta}}^+ &= \nu_{\bar{\eta}} \frac{u_\tau}{\nu} = \frac{u_\tau}{\nu} \left(\frac{D \nu^3}{4 u_b u_\tau^2} \right)^{1/4} \\ &= \left(\frac{D \nu^3 u_\tau^4}{4 \nu^4 u_b u_\tau^2} \right)^{1/4} \\ &= \left(\frac{1}{4} \frac{u_\tau}{u_b} \frac{D u_\tau}{\nu} \right)^{1/4} \\ &= \left(\frac{1}{2} \frac{u_\tau}{u_b} \frac{R u_\tau}{\nu} \right)^{1/4} \quad \text{with eq. (10)} \\ &= \left(\frac{1}{2} \frac{u_\tau}{u_b} R e_\tau \right)^{1/4} \end{aligned} \quad (16)$$

Table 1: Estimated mean Kolmogorov length scale $\sqrt{\bar{\eta}}$ for selected Reynolds numbers, where the ratio of Re to Re_τ is based on Blasius' empirical law. Length scales are given in inner and in outer units.

Re	Re_τ	$\sqrt{\bar{\eta}}^+$	$\frac{\sqrt{\bar{\eta}}}{R}$
5300	180.4	1.574	8.725×10^{-3}
11 700	360.7	1.826	5.062×10^{-3}
25 800	720.6	2.118	2.939×10^{-3}
59 600	1499.3	2.478	1.653×10^{-3}
130 000	2966.5	2.868	9.669×10^{-4}

for the mean Kolmogorov length scale expressed in inner units. Multiplying eq. (16) by eq. (10) we get an expression for the mean Kolmogorov length scale expressed in outer units (i.e. expressed in pipe radii R) in the form of

$$\begin{aligned}
\sqrt{\bar{\eta}}^+ \frac{1}{Re_\tau} &= \left(\frac{1}{2} \frac{u_\tau}{u_b} Re_\tau \right)^{1/4} \frac{1}{Re_\tau} \quad \text{with eq. (10)} \\
\sqrt{\bar{\eta}}^+ \frac{v}{u_\tau R} &= \left(\frac{1}{2} \frac{u_\tau}{u_b} Re_\tau \right)^{1/4} Re_\tau^{-1} \quad \text{with eq. (15)} \\
\sqrt{\bar{\eta}}^+ \frac{u_\tau}{v} \frac{v}{u_\tau R} &= \left(\frac{1}{2} \frac{u_\tau}{u_b} \right)^{1/4} Re_\tau^{1/4} Re_\tau^{-1} \\
\frac{\sqrt{\bar{\eta}}}{R} &= \left(\frac{1}{2} \frac{u_\tau}{u_b} \right)^{1/4} Re_\tau^{-3/4}. \tag{17}
\end{aligned}$$

References

- [1] H Blasius. *Das Aehnlichkeitgesetz bei Reibungsvorgängen in Flüssigkeiten*, pages 1–41. Springer Berlin Heidelberg, Berlin, Heidelberg, 1913. ISBN 978-3-662-02239-9. doi: 10.1007/978-3-662-02239-9_1. URL http://dx.doi.org/10.1007/978-3-662-02239-9_1.
- [2] Daniel Feldmann. *A numerical study on turbulent motion in oscillatory pipe flow*. Dissertation, Technische Universität Ilmenau, 2015. URL <http://www.db-thueringen.de/servlets/DocumentServlet?id=27407>.
- [3] Yosuke Hasegawa, Maurizio Quadrio, and Bettina Frohnäpfel. Numerical simulation of turbulent duct flows with constant power input. *Journal of Fluid Mechanics*, 750(2014):191–209, jul 2014. ISSN 0022-1120. doi: 10.1017/jfm.2014.269. URL http://www.journals.cambridge.org/abstract_S0022112014002699.
- [4] Stephen B. Pope. *Turbulent Flows*. Cambridge University Press, 7 edition, 2000. ISBN 978-0-521-59886-6.

- [5] Maurizio Quadrio, Bettina Frohnäpfel, and Yosuke Hasegawa. Does the choice of the forcing term affect flow statistics in DNS of turbulent channel flow? *European Journal of Mechanics - B/Fluids*, 55:286–293, jan 2016. ISSN 09977546. doi: 10.1016/j.euromechflu.2015.09.005. URL <http://arxiv.org/abs/1509.04877><http://dx.doi.org/10.1016/j.euromechflu.2015.09.005><http://linkinghub.elsevier.com/retrieve/pii/S0997754615200726>.
- [6] Friedemann Unger. *Numerische Simulation turbulenter Rohrströmungen*. Dissertation, Technische Universität München, 1994.